

# Experimental study of the convective plume above burning forest material

V.M. Sazanovich and R.Sh. Tsvyk

*Institute of Atmospheric Optics,  
Siberian Branch of the Russian Academy of Sciences, Tomsk*

Received September 17, 2001

A convective plume formed above some burning forest materials was investigated experimentally. The conditions of moderate and strong ground fire were modeled. Variances and spectra of intensity fluctuations and angles of incidence of a laser beam passing through the convective plume, as well as the altitude temperature distribution inside the plume were measured. The values of the structure characteristic of the refractive index inside the plume obtained from optical measurements and from measurements of the temperature gradient were compared.

## Introduction

Airflow, or a convective plume, arises above a ground forest fire due to the lift of heated products of the pyrolysis and burning of forest combustible materials (FCM). A convective plume is the main source of heat and aerosol particles from the fire zone to the atmosphere.<sup>1</sup> Characteristics of the medium in the plume formed due to buoyancy forces at heating by the burning layer of the FCM condensed phase and the spatially distributed burning gas phase depend on the fire intensity and the state of the atmosphere. Large vertical and horizontal temperature gradients achieving hundreds degrees per meter lead to the development of turbulent motion in the convective plume. The characteristics of this turbulent flow are almost unstudied.<sup>2</sup>

Mathematical simulations of forest fires need, as a rule, numerical integration of systems of nonlinear nonstationary three-dimensional equations of hyperparabolic type.<sup>1-4</sup> These systems of equations are solved numerically with the use of some assumptions and simplifications. In Ref. 2 it was noted that fluctuations of medium parameters in the fire zone cannot be calculated within the framework of the existing models of forest fires. At the same time, there exist a large number of principal problems that call for mathematical and physical simulation. For example,<sup>2</sup> the development of an improved mathematical model of a forest fire, techniques for numerical solution of three-dimensional problems for actual fires with the allowance for landscape, flow turbulence and its influence on the physical-chemical transformations proceeding in the fire zone (drying, pyrolysis, reaction of burning of gaseous and condensed combustible materials); allowance for the effect of mechanic vibrations of the FCM elements on their heat and mass exchange with the environment. The problems of numerical simulation of the flow formation in the convective plume are considered, for example, in Refs. 3 and 4.

In this paper, turbulent conditions in the convective plume arising above the burning forest material are studied experimentally with thermocouples by optical and thermal imaging methods. The burning conditions model a ground forest fire in the case of no wind. These studies are also interesting from the viewpoint of laser radiation propagation through a strongly turbulized medium layer.

## 1. Instrumentation and measurement techniques

Our experimental conditions simulated the conditions of a ground forest fire of a moderate (flame height  $0.5 < h < 1.5$  m) and strong ( $h > 1.5$  m) intensity at natural convection without wind. The experimental setup is shown schematically in Fig. 1.

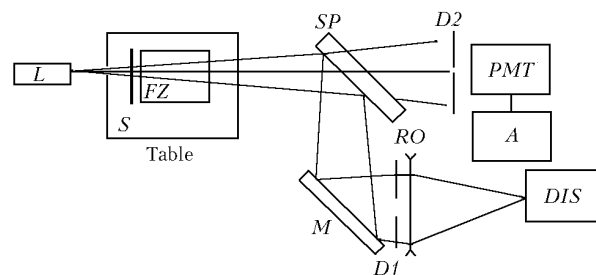


**Fig. 1.** Experimental setup: He-Ne laser *L*, flaming zone *FZ*; spiral *S*, semitransparent plate *SP*, mirror *M*, diaphragms *D1* and *D2*, photodetector of intensity fluctuations *PMT*, dissector meter of displacements *DIS*, and receiving objective *RO*.

The experiments were conducted on a 0.8×3.6 m table covered with a 200-mm thick soil layer and housed in a chamber of 10-m diameter and 28-m length that had two 600-mm diameter vents. The forest combustible material was placed uniformly over the flaming zone of 0.5×0.5 m area. As FCM, we used dry needles and

leaves of Siberian pine, pine, and birch. Besides, in some experiments we used dry 8-mm thick slats of Siberian pine. Slats were split into plates from 5 to 15 mm wide and stacked in a pile 40–50 mm high. The fire was initiated with an electric spiral placed along the FCM boundary.

In our experiments, to study the turbulent conditions in the plume, we used a divergent laser beam at the wavelength  $\lambda = 0.63 \mu\text{m}$ . The beam was close to the spherical wave. It passed through the plume at the height of 105 cm. Then it was divided into two beams by use of a parallel-sided plate. Intensity fluctuations were measured in one beam, and displacements of the source image were measured in the other one. A radiation source was separated by 5 m from a receiver and by 2.5 m from the fire zone. In most measurements, the flame front moved in the direction of the laser beam, thus providing for laser radiation propagation through the convective plume during the period of burning.

Intensity fluctuations were measured with a photomultiplier tube (PMT) preceded by a diaphragm  $D1$  of 0.15-mm diameter, i.e., much less than the expected inner scale of the turbulence. Image jitter fluctuations were measured simultaneously in the horizontal and vertical directions by a servo dissector system installed behind the receiving objective in the image plane. The focal length of the receiving objective was 500 mm, and the distance to the image plane was 550 mm. Changeable diaphragms  $D2$  of 7.8, 22, and 44 mm in diameter were installed in front of the receiving objective.

Analog signals from the PMT and dissector were amplified, digitized with a 12-bit ADC, and recorded in a computer. Simultaneously, the information was recorded using an NO67 7-channel analog recording magnetometer. Then the magnetometer data were entered into the computer with different discretization frequency. This technique allows calculation of correlation functions and time spectra of these signals in the frequency range from 0.05 Hz to 5 kHz. Computer processing of the data yielded variances, correlation functions, and spectra of intensity fluctuations and image displacements.

To measure the flame front propagation rate, we used the thermal imaging technique<sup>5</sup> based on the measurement of coordinates and determination of the velocity of the maximum temperature in the front.

The temperature distribution was determined by thermocouples of 0.1 mm in diameter installed in the zone of the convective plume (near the FCM center) at the heights  $z_i$  of 41, 72, 110, 150, and 180 cm above the substrate. Thus, as the flaming zone moves, the thermocouples measure the temperature distribution over the cross section of the fire front. The thermocouple signal was amplified, digitized with a 12-bit ADC, and recorded in the computer. The thermocouples were calibrated against the room temperature of 290 K, temperature of water in a thermostat from 303 to 363 K, and the temperature of melted pure tin at 505 K. Figure 2 depicts the calibration characteristic of one of the thermocouples.

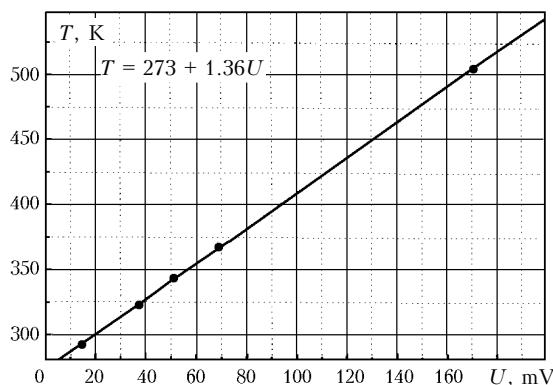


Fig. 2.

## 2. Measurement results

### 2.1. Thermal conditions in convective plume

For the convective plume above the flaming zone, the Rayleigh number is calculated from the measured temperatures at the height  $z$  of the beam axis:

$$\text{Ra} = \frac{g\beta z^3 \Delta T}{\nu\chi} \approx 10^{10},$$

where  $g$  is the acceleration of free fall;  $\beta$  is the volume expansivity of the medium;  $\Delta T$  is the temperature difference between the plume and the environment;  $\nu$  is the coefficient of kinematic viscosity;  $\chi$  is the thermal diffusivity.

Turbulent motion always exists in the medium at such values of the Rayleigh number.<sup>6</sup> The turbulent conditions in the atmosphere at free convection are determined by thermal factors. In this case, the statistical characteristics of the temperature field depend only on the parameters  $g/T_0$  and  $q/c_p\rho$ , where  $c_p$  and  $\rho$  are the thermal capacity and density of the medium;  $q$  is the heat flux density;  $T_0$  is the temperature at the initial height. Under these conditions, the height dependence of the temperature is described by the following equation<sup>6</sup>:

$$\begin{aligned} T(z) &= T_\infty + C_1 \left( \frac{q}{c_p \rho} \right)^{2/3} \left( \frac{g}{T_0} \right)^{-1/3} z^{-1/3} = \\ &= T_\infty + C_1 T_* z^{-1/3}, \end{aligned} \quad (1)$$

where  $C_1$  is a constant;  $T_\infty$  is the temperature at the infinity;  $T_*$  is the "thermal" complex of variables before  $z$ .

The temperature gradient is determined as

$$\frac{\partial T}{\partial z} = -\frac{C_1}{3} T_* z^{-4/3}. \quad (2)$$

The value of  $C_1 T_*$  should not depend on height under the same conditions of burning and heat generation and can be determined from the temperatures measured at two heights<sup>6</sup>:

$$C_1 T_* = C_1 \left( \frac{q}{c_p \rho} \right)^{2/3} \left( \frac{g}{T_0} \right)^{-1/3} = \frac{T(z_1) - T(z_2)}{z_1^{-1/3} - z_2^{-1/3}} \quad (3)$$

The results measured with thermocouples are exemplified in Figs. 3 and 4. The solid curves in Fig. 3a are the approximations of the temperature profile along the direction of front propagation at the heights  $z_i$  by the equation

$$T_{z_i}(x) = T_m e^{-\left(\frac{x-x_0}{a_T}\right)^2}, \quad (4)$$

where  $T_m$ ,  $x_0$ , and  $a_T$  are the maximum temperature value, coordinate of the maximum (time from the beginning of recording), and halfwidth of the temperature distribution in units of time (seconds). These parameters were fitted to the experimental data. At the known flame front propagation rate  $V$ , in cm/s, we can determine the plume halfwidth  $a_c = a_T V$ , in cm.

This approximation allows us to estimate the dimensions and position of the thermal plume, to analyze the height dependence of the mean maximum temperature, and to calculate the effect of turbulence on the parameters of the laser beam propagating through the plume.

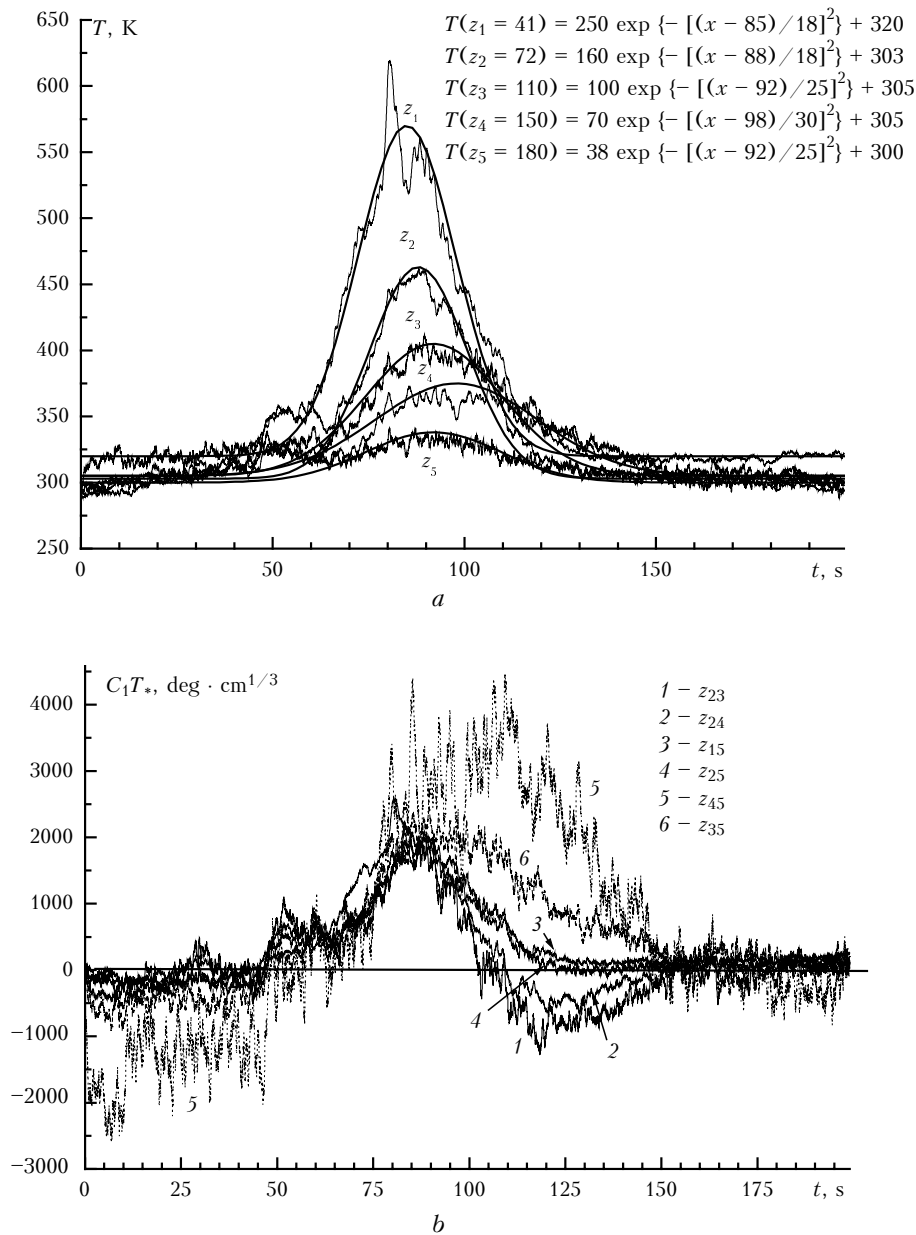
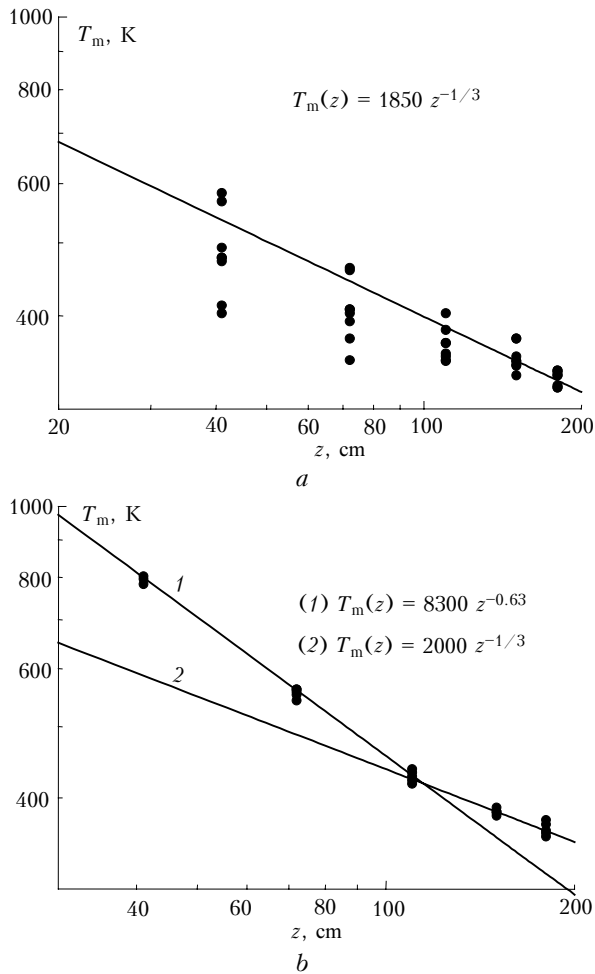


Fig. 3. Dynamics of the temperature  $T$  at different heights  $z_i$  (a) and the value of  $C_1 T_*$  calculated from gradients at different heights (b) at burning of Siberian pine needles.

Figure 4 depicts the dependence of  $T_m$  on the height  $z$  at burning of Siberian pine needles and birch leaves (fire of moderate intensity, flame height from 0.5 to 1 m) and Siberian pine slats (strong fire, flame height more than 1.5 m (Ref. 1)). The straight lines in Fig. 4b are calculated by the least-squares method, and those in Fig. 4a are obtained through fitting of the coefficients. It is seen from Fig. 4 that starting from some height, which depends on the burning intensity, the temperature in the convective plume decreases proportionally to  $z^{-1/3}$ . The values of  $C_1T_*$  calculated from the gradients between different heights vary insignificantly (see Fig. 3b).



**Fig. 4.** Height dependence of the maximum temperature: Siberian pine needles and birch leaves (a) and stacked Siberian pine slats (b).

Similar height dependences of  $T_m(z)$  and  $C_1T_*$  are characteristic of the conditions of free convection in the pure atmosphere. This suggests that turbulent conditions in the plume are similar to the turbulence in the atmosphere at free convection<sup>6</sup> and therefore Eqs. (1)–(3) can be applied to their estimation. At slat burning (see Fig. 4b), a zone of transition from burning FCM to the free convection area is present at the height lower than 100 cm. The temperature in this zone decreases

with height roughly as  $z^{-2/3}$ . According to the results of simultaneous thermal imaging measurements, the temperature of burning FCM is 1200–1400 K. Thermal imaging data evidence that similar transition zone is also observed at burning of Siberian pine needles and birch leaves. The height of this zone is only 10–15 cm. From Fig. 3b we can see some increase in  $C_1T_*$  values calculated at the heights of 110 and 150 cm with respect to the height of 180 cm ( $z_{35}$  and  $z_{45}$  are dashed curves). This increase is likely connected with the formation of an opposite ring flow near the plume. Similar flow arises at thermic floating-up in the atmosphere.<sup>7</sup> This is indicated by the opposite sign of the temperature and  $C_1T_*$  gradients near the plume in front of (at  $t < 50$  s) and in rear of the flame front (at  $t > 100$  s).

### 2.2. Calculation of $C_n^2$ from measured temperature gradients

As known, the structure function of temperature fluctuations in the atmosphere in the inertial interval of the turbulence spectrum is determined as<sup>8,9</sup>

$$D_t(r) = C_T^2 r^{2/3} \text{ for } l_0 < r < L_0,$$

where  $C_T^2$  is the structure characteristic of temperature fluctuations;  $l_0$  and  $L_0$  are the inner and outer scales of turbulence;  $r$  is the spread of observation points.

For the conditions of free convection,<sup>9</sup>

$$C_T^2 = C^2 a^2(\text{Ri}) \kappa^{4/3} z^{4/3} \left(\frac{\partial T}{\partial z}\right)^2, \quad (5)$$

where  $a^2(\text{Ri}) = 2.4$  is the function of the Richardson number,  $C^2 = 2.8$ , and  $\kappa = 0.4$  is the Von Karman constant.

For calculating  $C_T^2$ , we took the difference in the maximum temperature at the heights  $z_2 = 72$  cm and  $z_3 = 110$  cm that are close to the height of beam propagation. With the allowance for Eqs. (2), (3), and (5) and for the beam propagation height  $z_p = 105$  cm,  $C_T^2$  is (in  $\text{deg}^2 \cdot \text{cm}^{-2/3}$ ):

$$C_T^2 = 0.455 \Delta T_{2-3}^2$$

( $\Delta T_{2-3}$  is the measured temperature difference between the heights  $z_2$  and  $z_3$ ).

The structure characteristic of fluctuations of the air refractive index  $C_n^2$  ( $\text{cm}^{-2/3}$ ) is related to  $C_T^2$  by the equation, which has the following form for the laser radiation wavelength and particular temperatures<sup>8</sup>:

$$C_n^2 = \left(\frac{77.6 \cdot 10^{-6} p}{T^2}\right)^2 C_T^2 = (20.4 - 40.5) \cdot 10^{-13} C_T^2, \quad (6)$$

where  $T$ , in K, is the temperature at the selected height of 105 cm;  $p$  is the pressure, in mbar.

Thus, measuring the temperature at two levels under conditions of free convection, we can determine

the values of  $C_n^2$  and calculate the variance of image displacements  $\sigma_{\alpha p}^2$  for the source of spherical wave with the allowance for the size and position of the convective plume at the propagation path<sup>8,9</sup>:

$$\sigma_{\alpha p}^2 = 2.84 L(D)^{-1/3} \int_0^1 C_n^2(\xi) \xi^{3/5} d\xi. \quad (7)$$

In Eq. (7)  $L$  is the path length;  $D$  is the diameter of the receiving objective;  $C_n^2(\xi)$  is the  $C_n^2$  variation along the propagation path.

For calculating  $\sigma_{\alpha p}^2$  it was assumed that the coordinate dependence of  $C_n^2(\xi)$  is similar to the temperature distribution (4):

$$C_n^2(\xi) = C_{nm}^2 e^{-\left(\frac{\xi - \xi_c}{\xi_a}\right)^2},$$

where  $C_{nm}^2$  is the value at the maximum;  $\xi = x/L$  is the normalized path length;  $\xi_c$  and  $\xi_a$  are the distances from the radiation source to the plume center and the plume halfwidth (both normalized to the path length).

The Table gives the values of the temperature difference between the heights of 72 and 110 cm and the values of  $C_T^2$ ,  $C_{nm}^2$ , and  $\sigma_{\alpha p}^2$  calculated from them in different experiments. The last column of the Table presents the experimentally measured standard deviations of the image displacement for the laser beam  $\sigma_{\alpha exp} = (\sigma_{\alpha x}^2 + \sigma_{\alpha y}^2)^{1/2}$ , where  $\sigma_{\alpha x}$  is the horizontal component and  $\sigma_{\alpha y}$  is the vertical one.

Table. Measured and calculated results

FCM	$\Delta T_{2-3}^\circ$	$C_T^2$ , deg <sup>2</sup> ·cm <sup>-2/3</sup>	$C_{nm}^2$ , cm <sup>-2/3</sup>	$\sigma_{\alpha p}$ , arc. s	$\sigma_{\alpha exp}$ , arc. s
Siberian pine slats	140	11.9·10 <sup>2</sup>	17.3·10 <sup>-10</sup>	14.4	17.7, 23.5
	125	6.76·10 <sup>2</sup>	13.7·10 <sup>-10</sup>	14.05	15.9, 17.5, 21.2
	115	5.72·10 <sup>2</sup>	11.6·10 <sup>-10</sup>	16.2	26.3, 26.7, 27.3
	115	5.72·10 <sup>2</sup>	11.6·10 <sup>-10</sup>	11.8	15.3, 17.0,
Birch leaves	60	15.5·10 <sup>2</sup>	3.88·10 <sup>-10</sup>	16	20.1
	35	5.29·10 <sup>2</sup>	2.25·10 <sup>-10</sup>	13.2	21.3
	20	1.72·10 <sup>2</sup>	0.52·10 <sup>-10</sup>	4.7	14.0, 17.1, 14.7
	40	6.92·10 <sup>2</sup>	2.96·10 <sup>-10</sup>	10.9	9.8
	40	6.92·10 <sup>2</sup>	2.62·10 <sup>-10</sup>	7.7	8.4, 11.5

As can be seen from the Table, the measured standard (rms) deviations are close to the calculated ones, and this supports the conclusion about the similarity of turbulence in the convective plume and in the pure atmosphere.

### 2.3. Laser beam propagation through a convective plume

Figure 5 exemplifies the correlation functions of intensity fluctuations and image displacements for a laser beam. The form of the correlation functions is characteristic of the conditions of propagation in the turbulent atmosphere. The measured correlation functions were used for calculation of temporal frequency spectra with application of FFT.

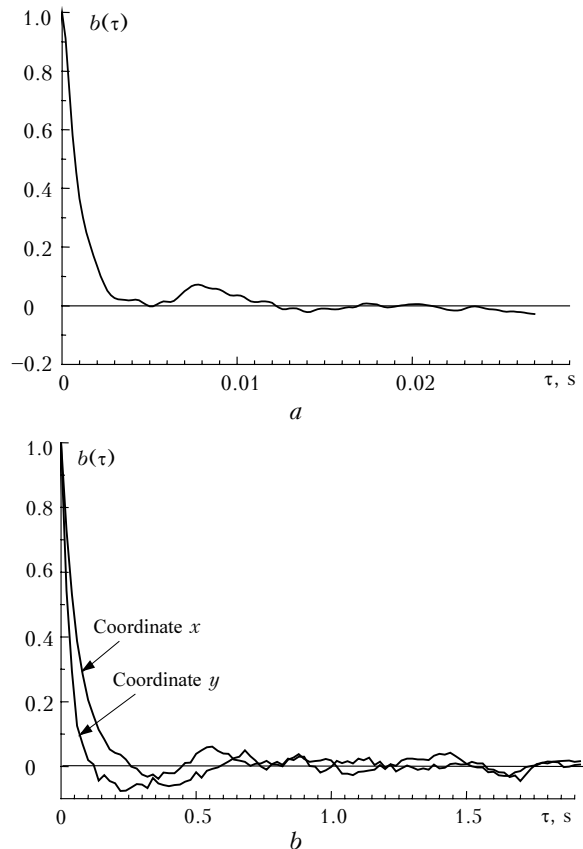


Fig. 5. Correlation functions of the intensity fluctuations (a) and image displacements (b).

As known (see, for example, Refs. 8 and 9), on the assumption of applicability of the “2/3” law and the hypothesis of frozen turbulence, the spectral density of power of image centroid fluctuations is a function of dimensionless frequency  $fD/V_{\perp}$  and is described by the following equation:

$$fW(f) = \frac{fW_1(f)}{\int_0^{\infty} W_1(f) df} = \text{const} \cdot \sin^2\left(\frac{\pi D}{V_{\perp}}\right) \left(\frac{fD}{V_{\perp}}\right)^{-5/3},$$

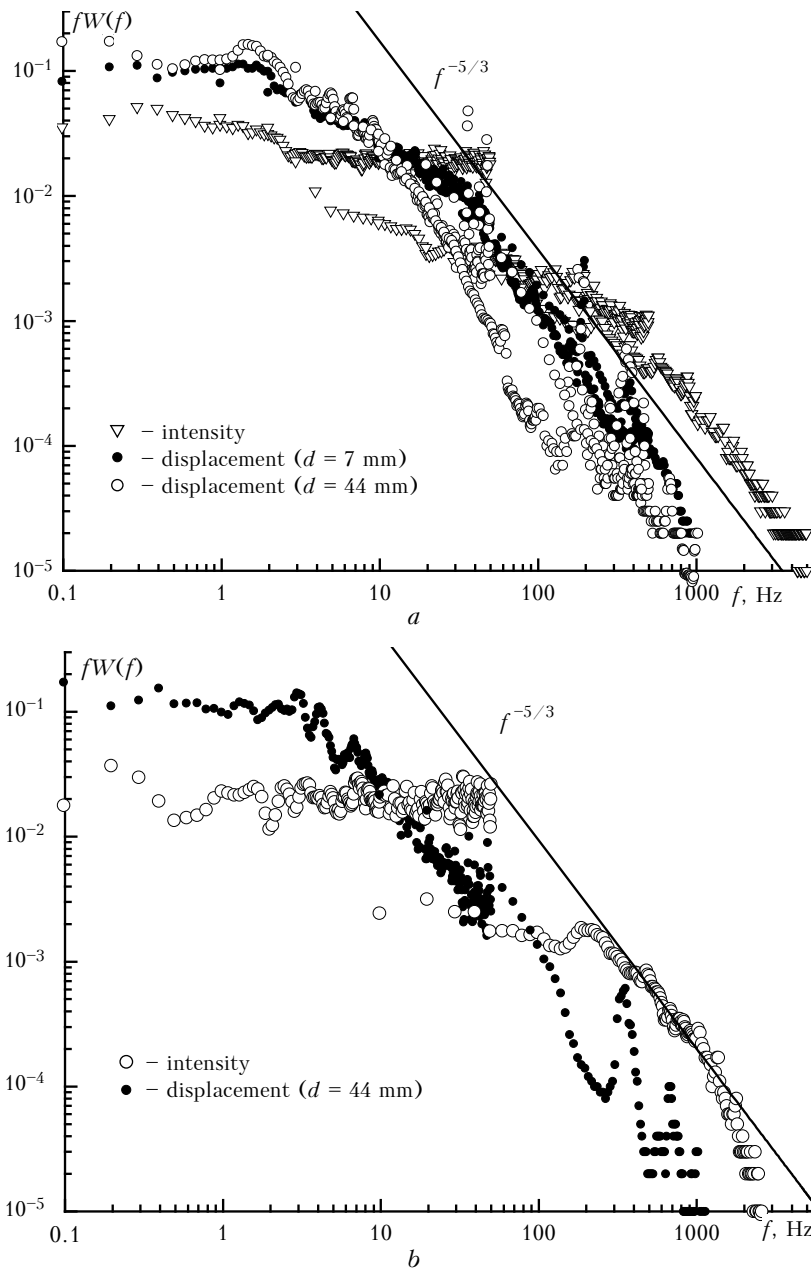
where  $V_{\perp}$  is the wind velocity component normal to the beam;  $W_1(f)$  is the measured spectrum.

Figure 6 presents the normalized spectra of intensity fluctuations and image displacements for two diaphragms at burning of Siberian pine slats and birch leaves. The straight lines correspond to the theoretical law of spectrum decrease  $\sim f^{-5/3}$  for the turbulent atmosphere.

It is seen from Fig. 6 that the spectrum of intensity fluctuations contains higher-frequency than the spectrum of fluctuations of the image displacements. One can see that the spectrum of fluctuations of the image centroid shifts to higher frequencies as the diaphragm of the receiving objective decreases (this fact is well known in the theory of wave propagation<sup>8,9</sup>). A rather large portion of the spectrum decreases as  $\sim f^{-5/3}$ . This is an evidence of the presence

of the inertial interval characteristic of atmospheric turbulence. In the region of high frequencies (higher than 50–100 Hz), the spectrum of image displacements has maxima and minima that are likely connected with the variation of the spectrum of temperature fluctuations in the region of small scales. The spectra of intensity fluctuations also have singularities at burning of Siberian pine slats, that is, under conditions of higher temperature gradients.

In the high-frequency region (higher than 1000 Hz), we can see a part of the spectrum with a faster decrease. This can be explained by a stronger effect of the dissipation interval with the increasing temperature gradient.



**Fig. 6.** Spectra of laser beam image displacements and intensity fluctuations at burning of birch leaves (a) and Siberian pine slats (b);  $d$  is the diameter of the diaphragm installed in front of the dissector.

Such a behavior of the spectrum is characteristic of the scales of the refractive index in the region of dissipation of turbulent energy, intensity fluctuations are sensitive to.<sup>8,9</sup> The difference in the spectra in the low-frequency region is connected with the processing technique, since the processing was performed using different discretization frequency and smoothing of the low frequencies (below the minimum one at the selected frequency). This allowed exclusion of their effect on the correlation function used for calculation of spectra while applying the FFT. The spectra are normalized, that is, the area under them is equal to unity. Therefore, extension of the spectrum to high-frequency region often leads to a decrease of the amplitude.

It should be noted that the spectra of vertical and horizontal components of centroid fluctuations are close to each other. This is likely indicative of the turbulence homogeneity within the scales  $\sim 10$  cm (two receiver dimensions). This conclusion is supported by the results of comparison of the standard deviations of fluctuations of image displacement along the horizontal  $\sigma_x$  and vertical  $\sigma_y$  coordinates (Fig. 7). The straight line in Fig. 7 is calculated by the least-squares method ( $R$  is the correlation coefficient).

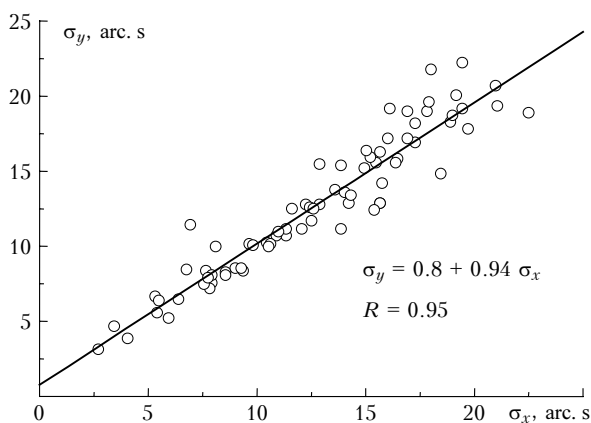


Fig. 7. Comparison of image displacements along the horizontal  $\sigma_x$  and vertical  $\sigma_y$  coordinates.

## Conclusions

The results obtained in studying turbulent conditions in the convective plume above a ground forest fire suggest the following conclusions.

Stating from some height  $z$ , the turbulent characteristics in the convective plume above the ground forest fire are close to the characteristics of atmospheric turbulence under conditions of free convection (the temperature decreases as  $\sim z^{-1/3}$ , and  $C_1 T_*$  changes only slightly). The height, from which these conditions are observed, is determined by the energy coming to the convective plume.

The intensity of temperature pulsations  $C_T^2$  and the refractive index  $C_n^2$  can be calculated from the measured

temperature gradients at two levels in the region of developed convection and from measured fluctuations of image displacements of a laser propagating through the convective plume by use of the equations for the turbulent atmosphere. Under conditions of moderate and strong ground forest fire,  $C_T^2$  at the maximum varies from  $10^2$  to  $10^3 \text{ deg}^2 \cdot \text{cm}^{-2/3}$  and  $C_n^2$  varies from  $5 \cdot 10^{-11}$  to  $2 \cdot 10^{-9} \text{ cm}^{-2/3}$ , what is three to five orders of magnitude higher than the maximum values in the atmosphere.

The measured variance of fluctuations of image displacements is close to that calculated from the temperature gradients with the allowance made for temperature distribution along the propagation path. The variances of the vertical and horizontal components are close. This indicates that the turbulence is homogenous on a  $\sim 10$ -cm scale (two receiver dimensions) under conditions of our measurements.

The spectrum of intensity fluctuations and image displacements of an optical wave have the frequency range, in which the spectrum  $fW_1(f)$  decreases as  $\sim f^{-5/3}$ , what corresponds to the inertial interval of the refractive index spectrum. In the spectrum of intensity fluctuations at a strong fire, there is an interval, in the region of high frequencies, where the spectrum decreases more sharply. Similar behavior of the spectrum in the atmosphere is caused by the effect of dissipation interval of the turbulence energy.

The vertical temperature gradients near the plume before and in the rear part of the flame front have the opposite sign, what indicates the presence of the opposite ring flow similar to that arising at thermic floating-up in the atmosphere.

## Acknowledgments

The authors are thankful to A.P. Rostov and A.L. Afanas'ev for the help in software development and to V.V. Reino, V.N. Krotenko, and M.V. Sherstobitov for the help in the experiment.

This work was partly supported by the Russian Foundation for Basic Research (Project No. 00-02-16747).

## References

1. A.M. Grishin, *Mathematical Simulation of Forest Fires and New Methods of Fire Control* (Nauka, Novosibirsk, 1992), 406 pp.
2. A.M. Grishin, in: *Selected Reports of the International Conference on Related Problems of Mechanics and Ecology* (Publishing House of the Tomsk State University, Tomsk, 2000), pp. 88-137.
3. L.Yu. Kataeva and E.M. Alekseenko, in: *Selected Reports of the International Conference on Related Problems of Mechanics and Ecology* (Publishing House of the Tomsk State University, Tomsk, 2000), pp. 174-190.
4. O.M. Belotserkovskii, M.N. Antonenko, A.V. Konyukhov, L.M. Kraginskii, and A.M. Oparin, in: *Proceedings of the*

*Fourth International Conference on Forest and Steppe Fires: Appearance, Propagation, Extinguishing, and Ecological Consequences* (Irkutsk, 2001), p. 22.

5. A.M. Grishin, A.A. Dolgov, V.V. Reino, R.Sh. Tsvyk, and M.V. Sherstobitov, *Atmos. Oceanic Opt.* **12**, No. 8, 691–694 (1999).

6. A.S. Monin and A.M. Yaglom, *Statistical Hydromechanics* (Nauka, Moscow, 1965), Part 1, 639 pp.

7. N.K. Vinnichenko, N.Z. Pinus, S.M. Shtemer, and G.N. Shur, *Turbulence in the Free Atmosphere* (Gidrometeoizdat, Leningrad, 1976), 288 pp.

8. V.I. Tatarskii, *Wave Propagation in a Turbulent Medium* (McGraw Hill, New York, 1961).

9. A.S. Gurvich, A.I. Kon, V.L. Mironov, and S.S. Khmelevtsov, *Laser Radiation in the Turbulent Atmosphere* (Nauka, Moscow, 1976), 277 pp.